Photophysics of (1-Butyl-4-(1*H*-inden-1-ylidene)-1,4-dihydropyridine (BIDP): An Experimental Test for Conical Intersections

Semyon Cogan, Anat Kahan, Shmuel Zilberg, and Yehuda Haas*

Department of Physical Chemistry and the Farkas Center for Light Induced Processes, the Hebrew University of Jerusalem, Jerusalem, Israel

Received: November 20, 2007; Revised Manuscript Received: March 7, 2008; In Final Form: March 7, 2008

Fluorescence experiments on (1-butyl-4-(1*H*-inden-1-ylidene)-1,4-dihydropyridine (BIDP) are reported in liquid and glassy solutions. The data indicate a fast decay in the fluid nonpolar, nonprotic solutions (decay times $\sim 10^{-12}$ s) and rapid but considerably slower decay in polar ones. In frozen solutions (polar and nonpolar), the fluorescence quantum yield is much higher (near 0.5 and around 0.1 in polar and nonpolar glasses, respectively). The rapid nonradiative transitions in fluid solutions are assigned to internal conversion in both solvent classes, as intersystem crossing is much slower and no net reaction is observed. These results are in agreement with predictions made for the closely related (in terms of electronic structure) but simpler molecule cyclopentadienyl-1,4-dihydropyridine (CPDHP) for which an S_1/S_0 conical intersection was recently proposed [*Int. J. Quant. Chem.* **2005**, *102*, 961]. The crossing of the two lowest singlet states is calculated to vanish in polar solvents such as methyl cyanide, leading to longer lifetime of S_1 of CPDHP. As BIDP has a very similar electronic structure, the model predicts a corresponding change in this larger molecule. The strong fluorescence observed in the glassy environments is rationalized by the hindering of the internal torsion required to reach the geometry of the conical intersection.

I. Introduction

Conical intersections (CIs), introduced to photochemistry by Teller in 1937,[1] received much attention in recent years mainly due to high level quantum mechanical calculations.[2] It turns out that conical intersections are commonly found in polyatomic molecules and are likely to be involved in many photochemical systems.[3] The theoretical effort to obtain structure and energy information of these degenerate loci on the potential surface of polyatomic molecules was matched by experimental work aimed at finding quantitative data that might confirm their presence.[4–7] The development of ultrafast experiments on the sub-picosecond time scale, provided a tool for quantitative estimates of the time for photochemical transformations in which CIs are believed (or computed) to be involved. However, only rather a few experimental tests in which the structure and energy of CIs were varied in a systematic or controlled manner have been reported to date. An example of recent important progress in the field is the probing of the excited state dynamics of uracil and its derivatives in several solvents.[8–10] The experimental data were interpreted in terms of the existence of conical intersections. In distinction with previous work, the use of several solvents (all polar) provided a means to control the energy level diagram of the system.

Several theoretical studies relate specifically solvent effects on CIs; only some highlights are mentioned here. Burghardt et al.[11] discussed the effects of electrostatic interactions on the CI within a dielectric continuum model. A solvent coordinate was introduced to explain the environmental impact on the location and character of the CI. Martinez and coworkers[12] used ab-initio results to re-parameterize a multi-reference semi-empirical method that reproduced the ground and excited state potential energy surfaces of large molecules (such as the chromophore of green fluorescent protein (GFP). Solvent effects on the energies of the relevant conical intersections were explored using a finite number of solvent molecules. This allowed the simulation of the photodynamics of the neutral GFP chromophore in both gas and solution phases. Improta and coworkers[13] proposed an explanation for the experimental significant solvent effect on the fluorescence lifetime of 5-fluorouracil in different solvents. They used time-dependent density-functional theory to explore the potential surface of the ground and excited states of uracil and similar molecules; the polarizable continuum model (PCM) was employed to take into account bulk solvent effects. The solvent was found to modulate the accessibility of an additional decay channel which is effective in acetonitrile but not in water. Garavelli and coworkers[14] also studied the properties of the green fluorescent protein chromophore in solution using ab-initio quantum-chemical calculations with the inclusion of solvent effects through PCM. The inclusion of solvent effects was crucial to reproduce correctly the activities of the anionic form. The structural effects of solvation are remarkable both in the ground and in the lowest excited state of the anionic chromophore and influence not only the vibrational activity but also the photodynamics of the lowest excited state. Rotation around the exocyclic CC double bond was shown to lead to a favored radiationless decay channel, more efficient than that in gas phase, explaining the ultrafast fluorescence decay and ground-state recovery observed in solution.

In this paper, we discuss the photo-physics of BIDP, a system for which an S_1/S_0 CI is predicted to be strongly affected by interactions with a solvent. In a previous publication,[15] the photo-oxidation of BIDP by molecular oxygen was reported. The oxidation is assigned to the reaction of the ground state molecules with singlet oxygen ($O_2(^1\Delta_g)$) which was produced in turn by energy transfer from the BIDP triplet state. The major deactivation process of the initially excited singlet after optical excitation turns out to be internal conversion (IC), whose rate constant is a few orders of magnitude larger than the rate

* Corresponding author. Fax: +97225618033

10.1021/jp7110296 CCC: $40.75 © 2008 American Chemical Society
Published on Web 05/30/2008

constants of intersystem crossing (ISC) and of fluorescence. The IC rate constant was predicted to be larger in nonpolar solvents than in polar ones, because of the existence of a conical intersection. Weak fluorescence was observed at room temperature in acetonitrile (MeCN, $\phi_f \sim 10^{-4}$), and none was observed in hexane. A tentative mechanism accounting for the small quantum yield of the fluorescence and of photo-oxidation was proposed. In this paper, we extended the fluorescence experiments to other solvents and to lower temperatures. In a glassy medium, the large amplitude motion required to reach the conical intersection geometry is inhibited, predicting higher fluorescence yields. This prediction was fully confirmed in the present work. The measured quantum yield of fluorescence may be used to calculate relevant rate constants from the proposed mechanism (eqs 1–4):

$$P(S_0) + h\nu \rightarrow P(S^*) \quad (1)$$

$$P(S^*) \rightarrow P(S_0) + h\nu \qquad k_f^0 \quad (2)$$

$$P(S^*) \rightarrow P(S_0) \qquad k_{IC} \quad (3)$$

$$P(S^*) \rightarrow P(T^*) \qquad k_{ISC} \quad (4)$$

The main deactivation process for the S_1 singlet state (denoted as P(S*)) is internal conversion whose rate constant k_{IC} was estimated[15] to be of the order of 10^{12} s^{-1}. On the basis of the experimental oscillator strength of the S_0-S_1 transition the radiative rate constant k_f^0 was estimated to be 1.3×10^8 s^{-1} in MeCN, and the intersystem crossing rate constant k_{ISC} was expected to be of the same order of magnitude as those for other substituted olefins.[16] Since $k_{IC} \gg k_{ISC}$ and also $k_{IC} \gg k_f^0$, the quantum yields of fluorescence, ϕ_f, can be approximated by $\phi_f = k_f^0/k_{IC}$. From the measured oscillator strength and fluorescence quantum yield, we estimated 3×10^{11} s^{-1} and 2×10^{12} s^{-1} for k_{IC} in MeCN and methylcyclohexane (MCH), respectively.[15] The faster rate obtained in a nonpolar is in accord with the existence of a conical intersection in nonpolar solvents, and the relatively small rate increase is due to the small separation between the two electronic surfaces in the nonpolar, of the order of 0.5 eV. In this paper, we report a more extensive study of the fluorescence and a more refined analysis of the absorption spectrum, which turns out to be composed of two transitions. Although some of the numerical values were modified by the more elaborate analysis, the main conclusions of the model are validated.

The theory used to locate a conical intersection using the Longuet–Higgins loop theorem was presented in previous communications.[17–19] The structures of the molecules studied in this work (1-butyl-4-(1*H*-inden-1-ylidene)-1,4-dihydropyridine (BIDP) as well as the smaller molecule used for high level computations (cyclopentadienyl-dihydropyridine (CPDHP)) are shown in Figure 1. The two dominant VB structures of BIDP are also shown; they are similar to those discussed for CPDHP in ref 17.

The quantum-mechanical calculations described in Section IV on the CPDHP model show that an S_1/S_0 conical intersection exists in the gas phase and in nonpolar solvents, whereas the degeneracy is removed in polar solvents. This unique property of CPDHP is assigned to the electronic structure at its equilibrium ground state configuration, namely, to the fact that the electronic wave function cannot be presented by single spin pairing scheme; rather, a covalent and a zwitterion forms are required. It is consequently found (ref 17) that there are two possible distinct routes on the ground state surface for the E-Z isomerization around inter-annular double bond. One is via the well-known biradical (covalent-ethylene-like) transition state, and the other is via a zwitterion (charge transfer) transition state that is stabilized by the concomitant aromatization of the two ring systems. The biradical transition state and the zwitterion transition states will be abbreviated by BRTS and ZWTS, respectively. As previously shown, a phase inverting Longuet–Higgins loop[17–19] can be constructed (Figure 2), in which a conical intersection is located.

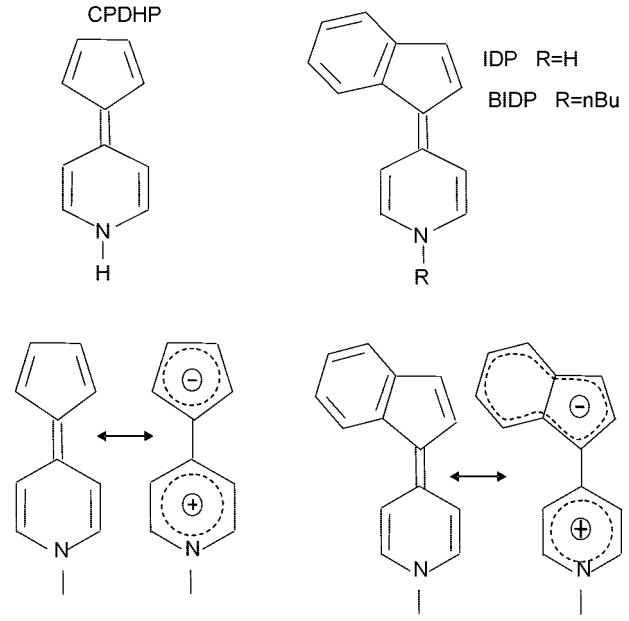

Figure 1. Structure of IDP, BIDP, and the model compound CPDHP. Top: molecular structure. Bottom: main VB structures.

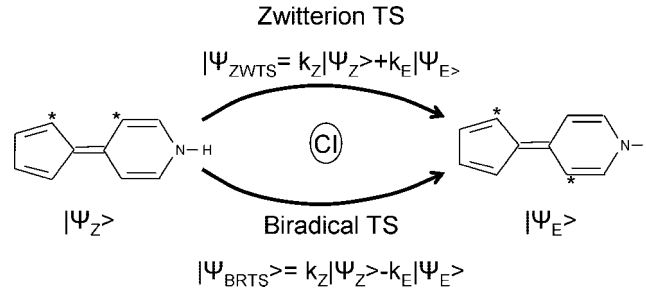

Figure 2. Two possible mechanisms of CPDHP E-Z isomerization. Together, they form a phase-inverting LH loop. The electronic wave functions $|\Psi_Z>$ and $|\Psi_E>$ were introduced and discussed in ref 17.

The structure and the energy of the conical intersection are closely related to both biradical and zwitterion transition states; in particular, the energy can be tuned by changing the solvent's polarity. In view of the similarity between the electronic structure of BIDP and that of CPDHP,[17] this deduction can be extended to BIDP.

This reasoning provided the motivation for the experimental work: we are interested in a molecular system in which the conical intersection can be manipulated in a pre-determined way. Calculations on CPDHP showed that whereas a conical intersection exists in nonpolar solvents, in polar solvents the separation between the S_0 and S_1 surfaces is around 0.5 eV even at the perpendicular geometry where the two states are closest to each other. Experimentally, the larger BIDP is much easier to handle; it is stable under ambient conditions, has a very strong absorption in the visible, and can be dissolved in both polar and nonpolar solvents. It was also reported to be nonfluorescent,[20] indicating rapid radiationless decay (the weak emission in MeCN reported below was discovered in the course of our

work[15]). For these reasons, BIDP was selected for the practical demonstration.

II. Experimental and Computational Details

BIDP was prepared and purified using literature procedures.[20] It was characterized by visible, IR, and NMR spectra. The solvents used were methylcyclohexane (MCH, Sigma-Aldrich, spectroscopic grade), 2-methyltetrahydrofurane (2MTHF, Sigma-Aldrich, >99%) and acetonitrile (MeCN, J. T. Baker, HPLC grade). Low temperature spectra were taken in 2MTHF and ethanol:isopentane:diethyl ether (EPA, 2:5:5) as polar solvents and methylcyclohexane:isopentane (MCHIP, 2:3) composition as a nonpolar solvent. All solvents used in the cryogenic experiments were obtained from Aldrich and were spectroscopic grade.

UV−vis absorption spectra in different solvents were recorded with HP 8452A photo-diode array spectrophotometer. Fluorescence spectra were recorded with Perkin Elmer LS50 luminescence spectrometer equipped with R928 photomultiplier. All spectra were corrected for the detector system response function (supplied by manufacture) and for the self-absorption of the sample.

For spectroscopic experiments at cryogenic temperatures, a home-made apparatus was used, built around an Oxford instruments double-wall cryostat equipped with a liquid nitrogen container and heating circuit operated by a temperature controller (Eurotherm Inc., model 2216L) . The white light source (Ocean Optics Inc., halogen−deuterium, UV-VIS-NIR DT-MINI-2-GS) and miniature spectrometer (Ocean Optics Inc., USB-4000) collinearly coupled through the cryogenic system by quartz fibers were used in absorption experiments. The same spectrometer with excitation source (CW-450 xenon high pressure lamp, Oriel Inc., model 6261) at perpendicular configuration was used in fluorescence experiments. The excitation wavelength was selected by passing the light beam through an interference filter (400 nm center wavelength, 40 nm FWHM). Prior to the measurements the solution was saturated with dry nitrogen gas to avoid photo-oxidation during spectroscopic experiments. The experimental setup allows the simultaneous measurement of absorption and emission spectra.

All calculations were performed with GAMESS[21] programs suite. The calculations for CPHDP were carried out at the MCSCF[22] (12, 11)/DZV[23] theory level. Some calculations were performed with a larger basis set (cc-pVDZ) for the perpendicular structures, yielding the same results. The active spaces for this included all of the π orbitals available (for perpendicular structures [4(b_1), 3(b_2), 4(a_2)] and planar [7(b_1), 4(a_2)]). Calculations for the larger IDP molecule (Figure 1) were performed at the B3LYP/cc-pVDZ level for the ground state and TD-DFT/B3LYP/cc-pVDZ for the excited state. The PCM or the reaction field approximations were used for the solvent effect simulation. Further details are specified in Section IV.

III. Experimental Results

IIIa. Absorption and Emission Spectra. The UV−visible absorption spectra of BIDP in several solvents and temperatures are shown in Figure 3. The poorly resolved vibrational structure noticeable at room temperature in MeCN and 2MTHF is strongly enhanced in the frozen solution. The absorption spectrum in the nonpolar glass MCHIP was of inferior quality at 83 K, possibly because of poor solubility.

IIIb. Emission Spectra and Fluorescence Quantum Yields. Fluorescence was found to be quite weak at room temperature. Figure 4 shows the emission spectra of BIDP in MCH and in

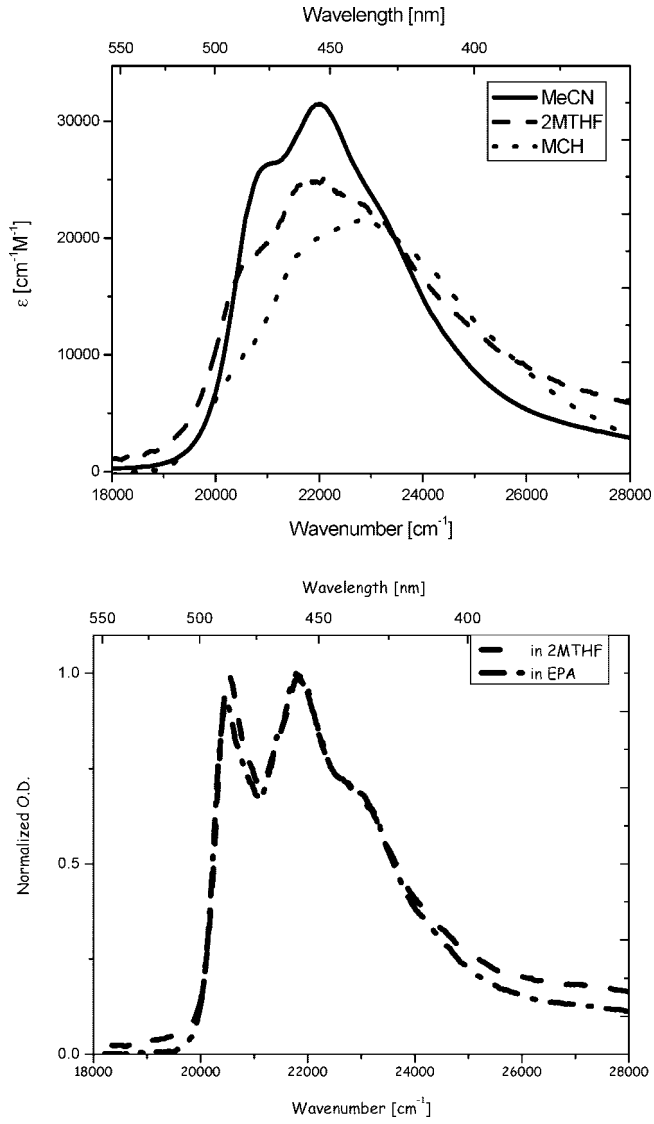

Figure 3. Visible−UV absorption spectrum of BIDP in MeCN, 2MTHF, and MCH at 298 K (top) and in 2MTHF and EPA at 83 K (bottom).

MeCN at room temperature; the Raman scattering of the solvent dominates the spectra, yet a very weak additional signal, assigned to fluorescence of BIDP, is seen in the MeCN solution. The fluorescence quantum yield in MeCN was measured with Coumarin 6 as the standard[24] to be $(4 \pm 2) \times 10^{-4}$. The rather large error bar is due to the weak signal and interference from the Raman scattering of the solvent. In MCH, as well as in hexane, no signal is observed above the noise level. Figure S1 (Supporting Information) compares the spectra in MeCN and that in the MCHIP mixture, when excitation was at 300 nm, allowing separation of the solvent Raman signal and the fluorescence. In this case, excitation is to a higher excited state, possibly involving other relaxation processes. However, as seen from the figure, no fluorescence is observed in the nonpolar solvent, whereas in MeCN, a clear fluorescence signal is recorded.

In frozen solutions, the fluorescence was strongly enhanced. The fluorescence excitation spectra coincided very well with the absorption spectra taken under the same conditions for 2MTHF. Figure 5 shows the absorption and emission spectra of BIDP in 2MTHF and in MCHIP at 83 K; under these conditions, fluorescence is seen to be quite intense. The quantum

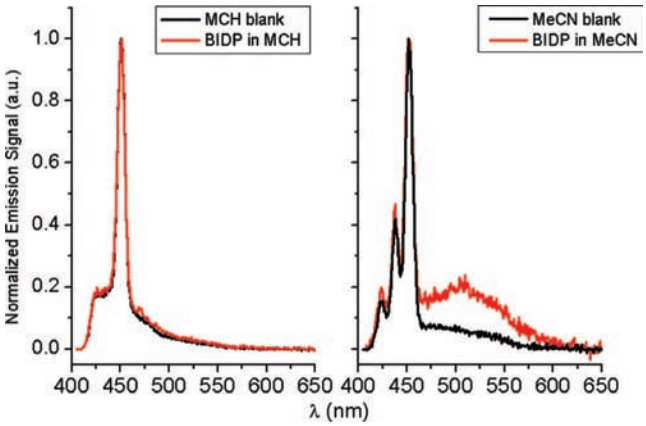

Figure 4. Emission spectra from BIDP in MCH (left, red) and MeCN (right, red) solutions measured at RT (298 K, excitation at 400 nm). The pure solvent spectra are shown in black. Raman scattering of the solvent is the dominant feature in both spectra, but in contrast to MCH solution in MeCN, an additional feature was detected, lying in the 480–600 nm wavelength region, assigned to the fluorescence of BIDP.

yields of BIDP fluorescence, measured at 83 K with R6G in methanol as a standard, are 0.23 ± 0.05 and 0.13 ± 0.05 in 2MTHF and MCHIP glasses, respectively. Table 1 and Figure 6 summarize the temperature dependence of BIDP fluorescence. Clearly, the yield is higher for the more polar solvents and steeply increases as the temperature is reduced.

The absorption spectrum of BIDP in MCHIP glass shown in Figure 5 is very different from the spectrum at room temperature, (Figure 3) and also from the spectra in the other glasses. Suspecting that the compound may undergo aggregation upon cooling because of its low solubility, we checked the fluorescence excitation of this glassy solution observed at several emission wavelengths. Some of the results are displayed in Figure S2 (Supporting Information). The spectra indicate that at least two different species fluoresce in this glass. The excitation spectrum of the emission around 525 nm is strongly reminiscent of the fluorescence in 2MTHF and is therefore assigned to monomeric BIDP. When the emission was monitored at 625 nm, a very different excitation spectrum was obtained. The absorption spectrum appears to be a superposition of these two excitation spectra. Warming the glass to room temperature recovered the normal room temperature spectrum, and the process could be repeated indefinitely. As there was no sign of a chemical change, a likely explanation is that the species giving rise to the 625 nm emission is a dimer or some other aggregate of BIDP. Its exact nature was not further pursued, as our main purpose in this work was in the monomer molecule. Indirect evidence supporting this assumption is the fact that, in contrast with the case of polar solvents, we were not able to fit the BIDP absorption spectra in MCHIP at low temperatures using the method described in the next subsection (IIIc).

In an attempt to detect possible aggregation effects on the absorption spectrum at room temperature, the concentration of BIDP was varied between 3×10^{-7} M and 1×10^{-5} M. As seen from Figure S3 (Supporting Information); Beer's law appears to be obeyed and no change in the spectrum was observed.

IIIc. Analysis of the Absorption Spectra. The spectra were analyzed using the method of Heller et al.,[25] further developed by Myers and Mathies.[26] The simulation of the spectrum is based on eq 5, assuming the Born−Oppenheimer and the Condon approximations.

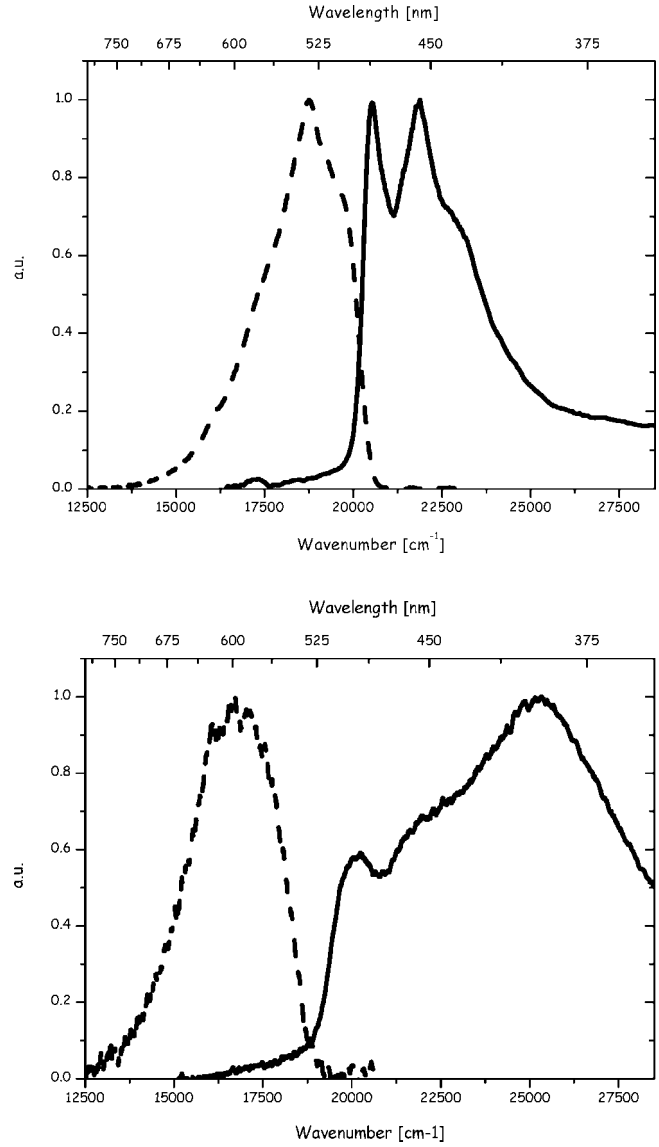

Figure 5. Low temperature, 83 K, absorption and fluorescence spectra of BIDP in 2MTHF (top) and MCHIP (bottom).

TABLE 1: Fluorescence Quantum Yields As a Function of Solvent and Temperature

	MCHIP	2MTHF	MeCN[a]
Φ_{fl}, 83 K	0.13 ± 0.05	0.23 ± 0.02	0.59
Φ_{fl}, 103 K	0.005 ± 0.001	0.081 ± 0.008	0.30 ± 0.02
Φ_{fl}, 133 K	0.002 (123 K)	0.003 ± 0.001	0.01

[a] Used Coumarine 6 as a standard and measured at front surface setup.

$$\sigma_A(E_L) = \frac{4\pi^2 e^2 M^2 E_L}{3\hbar cn} \sum_{\nu} \frac{\Gamma}{\pi} \frac{|<\nu|i>|^2}{(\varepsilon_\nu - \varepsilon_i + E_0 - E_L)^2 + \Gamma^2} \quad (5)$$

In eq 5, $\sigma_A(E_L)$ is the absorption cross section from the level $|i>$, e is the charge of the electron, η is Planck's constant, c is the velocity of light, n is the refraction index of the solvent, Γ is the homogeneous line width, E_0 is the energy separation between the lowest vibrational level of the ground state and the electronic excited state, E_L is the energy of the incident photon, and ϵ_ν and ϵ_i are the energies of the vibrational level $|\nu>$ in the excited state and $|i>$ in the ground state. M is the electronic transition length (Å) between the ground electronic state and the excited state, and $|<\nu|i>|^2$ is

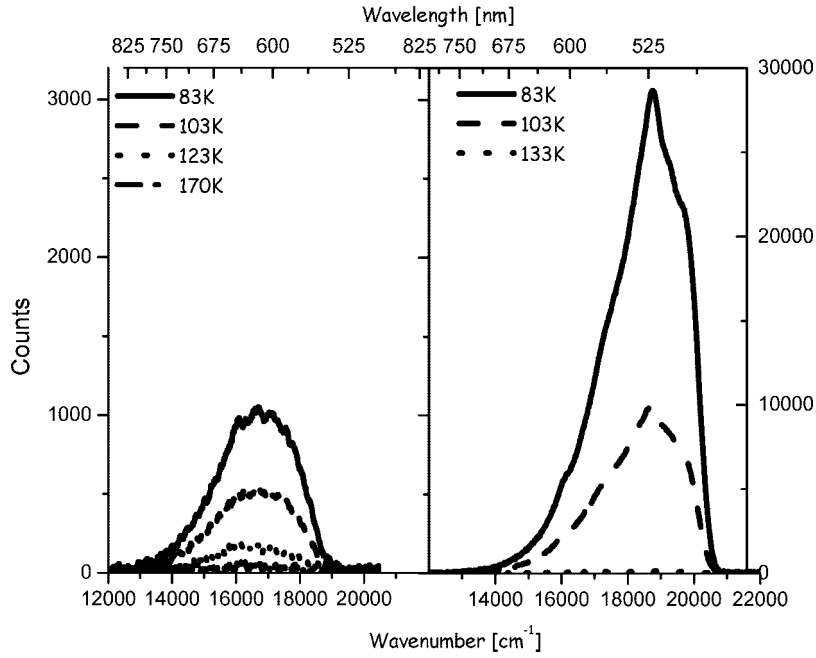

Figure 6. Temperature effect on the fluorescence of BIDP in MCHIP (left) and 2MTHF (right). The spectra were taken in the same cell under identical conditions, excitation at 400 nm.

the Franck Condon factor. Energies and widths are expressed in cm^{-1} units.

This expression can be used to calculate the absorption cross section provided the FC factors are known. A simple approximation is the displaced harmonic oscillator model, which is useful for large molecules; it assumes harmonic frequencies, negligible change in the frequencies of the normal modes between the two electronic states, and an origin shift Δ in dimensionless normal coordinates. Only modes in which Δ is large contribute to the spread of the observed absorption spectrum. Each vibronic component is broadened inhomogenously (mostly due to different sites at low temperature or to thermal occupation of different levels at high temperatures). A simple approximation is to add a width θ to each band assuming Gaussian distribution:

$$\sigma_{i\rightarrow j}(E_L)\alpha\frac{1}{W}\int_0^\infty dE_0 \exp\left[\frac{-(E_0-\overline{E_0})^2}{2\theta}\right]\times \sum_\nu \frac{\Gamma}{\pi}\frac{|<\nu|i>|^2}{(\varepsilon_\nu-\varepsilon_i+E_0-E_L)^2+\Gamma^2} \quad (6)$$

By using the time-domain approach of Heller and coworkers, the expression for the absorption cross section becomes[25,27]

$$\sigma_A(E_L)=\frac{4\pi^2e^2M^2E_L}{3\hbar cn}\int_{-\infty}^{\infty}\exp[i(E_L-V)t/\hbar]x\exp(-\Gamma|t|/\hbar)\times \prod_{n=1}\exp\{-s_n[1-\exp(-i\omega_n t)]\}dt \quad (7)$$

where $s_n = \Delta^2/2$ and ω_n is the frequency of the n mode in the excited state.

Attempts to analyze the spectra assuming a single absorption band failed. An insight into the underlying energy level diagram was obtained by calculations using the PCM-TD-DFT/B3LYP method on the parent molecule IDP, summarized in Table 2.

As seen from the table, four electronic states are predicted in the relevant 3 to 4 eV energy range, of which only two have large oscillator strength. We therefore assumed that the absorption spectra are composed of two overlapping transitions due to the S_0-S_1 and S_0-S_3 transitions. In the simulations, eq 3 was employed for both electronic transitions and applied to spectra measured at 83 K and at room temperature. Some representative simulations are shown in Figure 7, and the data are tabulated in Table 3. The parameters used to obtain the best fits are summarized in Table 4.

TABLE 2: Calculated Energies of the Low Lying Excited Singlet States of IDP in the Franck−Condon Region (Electronvolts Relative to the Ground State Minimum) and the Oscillator Strengths of the Corresponding Transitions Using PCM-TD-DFT/B3LYP for Solvents with Different Dielectric Constants (ϵ)[a]

state	ϵ	energy, eV	calculated $f(S_0-S_i)$
S_1	1.0	3.1	0.15
	2.0	3.1	0.54
	37.5	3.2	0.69
S_2	1.0	3.2	0.003
	2.0	3.3	0.005
	37.5	3.5	0.005
S_3	1.0	3.5	0.50
	2.0	3.4	0.33
	37.5	3.6	0.16
S_4	1.0	4.0	0.07
	2.0	4.1	0.05
	37.5	4.0	0.06

[a] ϵ =1, 2, and 37.5 simulate gas phase, nonpolar, and polar solvents, respectively.

The simulation was very sensitive to the parameters Γ and Δ and the homogeneous line-widths. The three vibrational frequencies used were chosen as representing modes well-known to be active in the UV spectra of aromatic compounds.

The resulting experimental oscillator strengths (f) were used to derive the radiative lifetimes (τ_o) and the radiative rate constants ($k_f^0 = 1/\tau_o$) using the Strickler−Berg equation[28] (8).

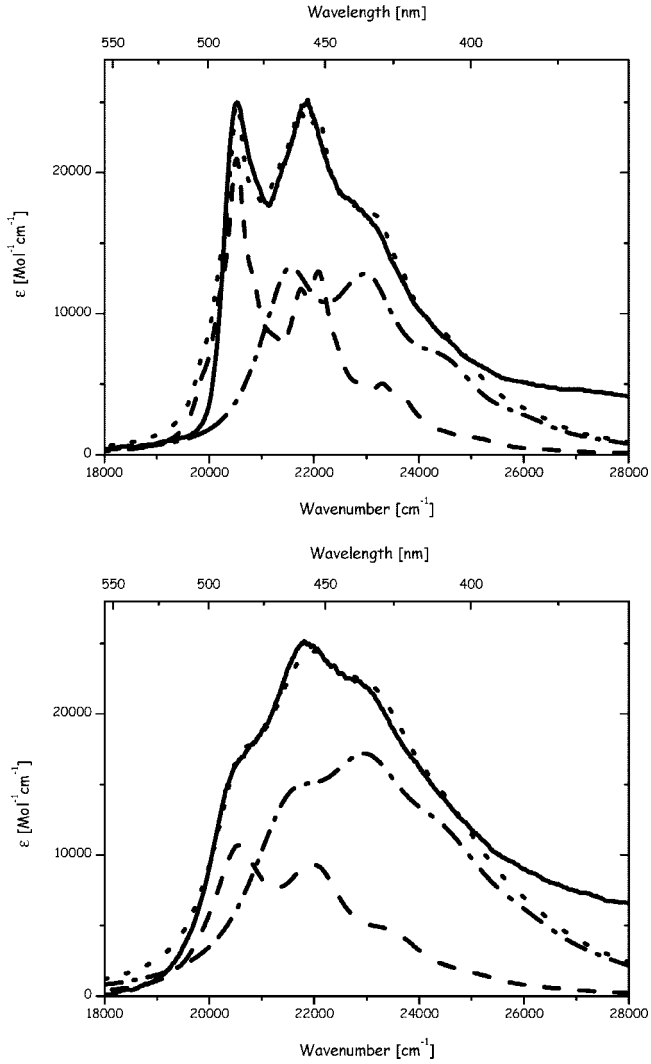

Figure 7. Examples of the simulations of absorption spectra in MTHF at 83 K (top) and at 298 K (bottom). Full line: experimental data. Dashed line: simulation of the S_0-S_1 transition. Dot-dashed line: simulation of the S_0-S_2 transition. Dotted line: simulation of the whole spectrum by combining the simulated S_0-S_1 and simulated $S-S_2$ transitions. The parameters used for the simulation are listed in Table 4.

$$\frac{1}{\tau_0} = k_f^0 = A = 8 \cdot 2303\pi c\langle \nu_{em}^{-3}\rangle^{-1} n^2 N_A^{-1} \int \varepsilon d\ln\nu \qquad \text{and}$$

$$f = \frac{2\pi\varepsilon_0 mc^3}{\nu^3 e^2} A \quad (8)$$

The oscillator strengths at room temperature $f_{S_0\text{-}S_1}$, RT and $f_{S_0\text{-}S_3}$, RT (Table 3, rows 4 and 5) are obtained from the analysis of the absorption spectra (Figure 7); k_f^0, RT (rows 6 and 7) are derived from $f_{S_0\text{-}S_1}$. τ_f, the fluorescence decay time at 83 K, is estimated from the measured fluorescence quantum yield $\Phi_{fl,83K}$ (Table 1) and τ_0 using $\tau_f = \Phi_{fl,83K} \cdot \tau_0$. τ_0 is assumed not to be independent of the temperature.

Inspection of Table 3 shows that the oscillator strengths of the two transitions giving rise to the absorption spectrum are indeed quite large. They (as well as the transition energies) compare qualitatively well with the theoretically predicted ones (Table 2), although the measured S_0-S_1 transition has a smaller oscillator strength than the calculated one for both the polar and the nonpolar solvents (by a factor of 3). In view of the limited prediction accuracy of oscillator strengths, this result indicates satisfactory agreement with the model calculations.

IV. Solvent Effects − Theory: Role of Conical Intersections. ***Computational Results on the CPDHP Model System.*** The thermal E/Z isomerization of CPHDP and BIDP belongs to a class of reactions for which two different routes are possible; as discussed in the Introduction, this situation leads to a conical intersection between the two lowest singlet states (S_0 and S_1). The observed fast decay of the excited singlet state of BIDP at room temperature and the very weak fluorescence, as well as the solvent dependence of this efficient radiationless process are compatible with the existence of an S_1/S_0 conical intersection. Detailed computations of the properties of the system in different solvents were carried out on CPDHP, whose smaller size allowed a rather high level of theory.

The critical points of CPDHP were optimized at the MCSCF (12,11)/DZV theory level under C_{2V} symmetry point group restrictions (this restriction was justified by the results as discussed below). The effect of the solvent was approximated using the self consistent reaction field (SCRF) theory in the framework of the Kirkwood−Onsager[29,30] and PCM[31] models.

Comparison of the two solvation models was made for two representative solvents, cyclohexane and acetone. As can be seen from Table S1 (in Supporting Information), the two models give practically the same results. Consequently, the simpler Onsager model was used for estimating the effect of the solvents, as summarized in Table 5.

In the isolated molecule (gas phase), a single critical point was found at the planar nuclear configuration whose electronic wavefunction is of A_1 symmetry; this proved to be the global minimum as verified by vibrational analysis. Two different transition states (one of A_1 and the other A_2 symmetry), were found on the ground state potential energy surface lying at 2.17 and 1.91 eV above the planar minimum; both are of a perpendicular nuclear configuration (see Figure S4 in Supporting Information), and vibrational analysis showed that both structures are transition states, having each a single imaginary root. These structures were identified as the ZWTS and BRTS used by the model to find the CI, on the basis of their calculated dipole moments, 16 and 2 Debye, respectively.

Further calculations on these systems were performed also at the MP2-MCSCF (12/11)/DZV level on the MCSCF optimized structures at the geometry of the transition states, in order to check for possible electron dynamic correlation effects, which are especially important for charge transfer states. As summarized in Table S2, the application of the MP2 correction on MCSCF structures generally lowers the total energies of all of the structures, yet the relative energy of the biradical transition state with respect to the global minimum structures changed only slightly (0.07– 0.18 eV at different geometries), whereas the effect on the zwitterion states is considerably larger (0.5–0.8 eV at different geometries). At the MP2 level, the two transition states were found to have approximately the same barrier (1.7 eV). The energy of the first excited singlet state at the geometry of the BRTS was found to be a mere 0.13 eV higher than that of ground state. A considerably larger energy gap was found for the ZWTS, approximately 0.5 eV.

A conical intersection was found on the coordinate that connects linearly the two transition states along aromatization coordinate,[32] (Figure 8), using the method previously described in detail.[17,19] The conical intersection was found to lie near the higher transition state. As the conical intersection of CPDHP is found inside a loop involving two transition states of very different polarities, its energy is expected to be affected by external electric fields.

TABLE 3: Molecular Constants Derived from the Absorption and Emission Spectra of BIDP in Several Solvents

	units	MCHIP	2MTHF	MeCN
ϵ, dielectric constant		2.02[a]	6.97[a]	35.94[a]
melting point/glass point	K	146[c]	137[b]	229[a]
ϵ, extinction coefficient	cm^{-1} M^{-1}	21600 @ 438 nm	25200 @ 458 nm	30600 @ 454 nm
ν0–0 (S_0-S_1)	eV	2.59	2.54	2.58
ν0–0 (S_0-S_3)	eV	2.70	2.66	2.70
fs_0-s_1, RT		0.14	0.20	0.26
fs_0-s_3, RT		0.23	0.39	0.22
k_f^0, RT (A_{01})	sec^{-1}	4.06×10^7	5.58×10^7	7.60×10^7
τ_0 ($= 1/k_f^0$)	sec	24.6×10^{-9}	17.9×10^{-9}	13.2×10^{-9}
$k_{isc} + k_{ic}$, 83 K[c]	sec^{-1}	3.65×10^8	1.87×10^8	5.28×10^7
Φ_{fl}, RT				4×10^{-4}
k_{fl} ($= k_{ic}$)[d]	sec^{-1}	1.8×10^{12}		3.6×10^{11}
τ_f ($= 1/k_{fl}$)	sec	5.5×10^{-13}		2.78×10^{-12}
$\tau_{f,expected}$, $\Phi_{fl,83K} \cdot \tau_0$ [e]	sec		4.12×10^{-9}	7.79×10^{-9}

[a] From the *Handbook of Photochemistry*, 2nd ed., S. L. Murov, I. Carmichael, G. L. Hug, Dekker: New York, 1993. [b] D. F. Aycock, *Org. Proc. Res. Dev.* **2007**, *11*, 156–159. [c] Using $\Phi_{fl>} = k_{fl}/(k_{fl} + k_{isc} + k_{ic})$ and assuming the rate constants for MCHIP and MCH are very similar. [d] The calculated actual fluorescence decay rate constant, equal approximately to the internal conversion rate constant. [e] The expected measured lifetime at 83 K.

TABLE 4: Parameters Used in the Spectral Analysis of the Absorption Spectra[a]

	E_L [cm^{-1}]	Γ [cm^{-1}]	M [Å]	Δ_1	Δ_2	Δ_3	θ [cm^{-1}]	n
MeCN, 298 K	20840 ± 50	110 ± 5	1.26 ± 0.03	0.70 ± 0.04	0.65 ± 0.06	0.70 ± 0.07	350 ± 35	1.344
	21800 ± 30	125 ± 15	1.21 ± 0.03	0.70 ± 0.05	0.70 ± 0.05	0.70 ± 0.07	350 ± 35	1.344
2MTHF, 83 K	20520 ± 10	50 ± 7	1.06 ± 0.02	0.68 ± 0.04	0.65 ± 0.1	0.73 ± 0.07	330 ± 10	1.406
	21500 ± 80	120 ± 15	1.18 ± 0.04	0.78 ± 0.07	0.79 ± 0.07	0.76 ± 0.02	330 ± 10	1.406
2MTHF, 298 K	20520 ± 10	100 ± 15	1.00 ± 0.02	0.78 ± 0.04	0.66 ± 0.04	0.80 ± 0.05	330 ± 10	1.406
	21500 ± 30	190 ± 20	1.50 ± 0.05	0.89 ± 0.05	0.80 ± 0.05	0.90 ± 0.06	330 ± 10	1.406
MCH, 298 K	20900 ± 10	90 ± 10	1.00 ± 0.02	0.76 ± 0.04	0.69 ± 0.04	0.92 ± 0.06	400 ± 10	1.423
	21840 ± 80	125 ± 15	1.35 ± 0.05	0.94 ± 0.06	0.9 ± 0.06	0.91 ± 0.06	400 ± 10	1.423

[a] The same three vibrational frequencies were used for both the simulation, with frequencies $\upsilon_1 = 1640 \pm 40$ cm^{-1}, $\upsilon_2 = 1530 \pm 30$ cm^{-1}, and $\upsilon_3 = 1190 \pm 20$ cm^{-1}. The corresponding Δ values are shown in the table.

TABLE 5: Calculated Energies of Some Critical Points of CPDHP (MCSCF(12,11)/DZV) Using the Kirkwood−Onsager[29,30] Approximation[a]

structure medium	global minimum	biradical TS (when relevant)* [b]	Zwitterionic TS	conical intersection
medium				
gas Phase $\epsilon = 1.0$	1^1A_1 **-438.325196** [0] (4.0 D)	1^1A_2 [1.91] (2.0 D) 1^1A_1 [2.52] (16.5 D)	1^1A_1 [2.17] (16.9 D) 1^1A_2 [2.26] (2.1D)	[2.24]
cyclohexane $\epsilon = 2.02$	1^1A_1 **-438.326204** [0] (4.7 D)	1^1A_2 [44] [1.91] (2.2 D) 1^1A_1 [2.09] (18.7 D)	1^1A_1 [1.74] (19.1 D) 1^1A_2 [2.26] (2.4 D)	[1.96]
trichloro- ethylene $\epsilon = 3.0$	1^1A_1 **-438.326892** [0] (5.25 D)	1^1A_1 [1.83] (19.9 D) 1^1A_2 [1.96] (2.3 D)	1^1A_1 [1.48] (20.4 D) 1^1A_2 [2.30] (2.5 D)	n.a.
bromoform $\epsilon = 4.4$	1^1A_1 **-438.327189** [0] (5.5 D)	1^1A_1 [1.74] (20.5 D) 1^1A_2 [1.96] (2.3 D)	1^1A_1 [1.35] (20.9 D) 1^1A_2 [2.30] (2.6 D)	n.a.
methyl ether $\epsilon = 5.0$	1^1A_1 **-438.327323** [0] (5.6 D)	1^1A_1 [1.70] (20.7 D) 1^1A_2 [1.96] (2.4 D)	1^1A_1 [1.30] (21.2 D) 1^1A_2 [[2.30] (2.6 D)	n.a
acetone $\epsilon = 20.7$	1^1A_1 **-438.328266** [0] (6.4)	1^1A_1 [[1.36] (22.11D) 1^1A_2 [1.97] (2.5 D)	1^1A_1 [1.00] (22.7 D) 1^1A_2 [[2.35] (2.8 D)	n.a
acetonitrile $\epsilon = 37.5$	1^1A_1 **-438.328431** [0] (6.5 D)	1^1A_1 [1.30] (22.3D) 1^1A_2 [1.96] (2.5 D)	1^1A_1 [1.00] (22.9 D) 1^1A_2 [2.35] (2.8 D)	n.a.

[a] Bold, absolute energies in Hartree units; square brackets [], relative energy in eV; brackets (), dipole moment. [b] The biradical TS (1^1A_2 symmetry) was found only in the gas phase and in cyclohexane. In the other solvents, the 1^1A_2 state is part of S_1.

It can be readily seen (Figure 8) that the stabilization of the zwitterion transition state upon solvation (in the nonpolar solvent compared with the gas phase) not only decreases the energy of the S_0/S_1 conical intersection energy but also moves the crossing point toward the geometry of the higher lying biradical transition state. This result resembles Hammond's postulate[33] for transition states of thermal reactions: the structure of a transition state is similar to that of the species nearest to it in free energy; in other words, the transition state structure resembles the less stable minimum. On the basis of these findings, we postulate an analogue for Hammond's postulate for photochemical reactions: the conical intersection structure is similar to that of the less stable transition state in the relevant LH loop. Whereas the energy minima (reactant and product) are the reference structures in the original Hammond postulate for the transition state, in the case of conical intersections, the reference structures are transition states themselves. As the greater stabilization of the charge transfer state in a polar solvent eliminates the biradical TS on ground potential energy surface (it becomes a species on the excited state surface), no Longuet−Higgins loop can be formed using the E-Z isomerisation channels through biradical

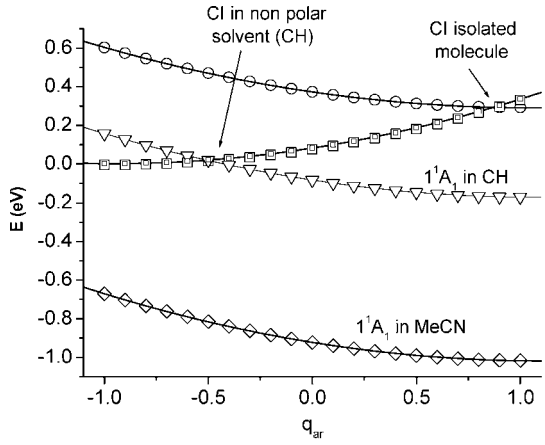

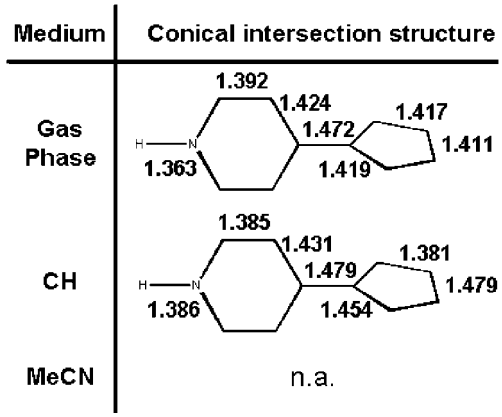

Figure 8. Calculated solvent effects on the conical intersection of CPDHP (MCSCF(12, 11)/DZV), Kirkwood−Onsager approximation. Top: The energies (relative to the energy of the biradical transition state at its minimum) of the zwitterion and biradical states in different solvents along the coordinate that connects linearly the two transition states. It is termed the aromatization coordinate Q_{ar} as it transforms the two rings from the olefinic form of the biradical TS to the aromatic structure of the zwitterion TS. Q_{ar} is defined by the expression: $Q_{ar} = 1/2(Q_{BRTS} + Q_{ZWTS}) + 1/2(Q_{ZWTS} - Q_{BRTS}) \cdot q_{ar}$ (Q_x is the collection of the Cartesian coordinates of species x). q_{ar} is a scalar that varies between -1 and 1 such that at $q_{ar} = -1$ the geometry is that of the BRTS, and at $q_{ar} = +1$ it is the geometry of the ZWTS. The energy of biradical state (1^1A_2, squares) remains essentially unaltered by the interaction with all solvents (therefore, only one graph is shown), whereas the energy of the zwitterion state (1^1A_1) is stabilized by the solvents (circles- isolated molecule, triangles- in cyclohexane (CH), diamonds- in acetonitrile (MeCN)). In MeCN, the 1^1A_2 is an excited state for all values of q, and no crossing between the two states is possible. Note that in this figure only one of the two coordinates leading from the ground state to the conical intersection is shown. The second is the torsion coordinate, which is kept at 90° in this cut. Compare Figure 2 and Figure 6 of ref 15. Bottom: The structure of the conical intersection in the gas phase (top) and in cyclohexane (middle). No conical intersection was located in MeCN.

and zwitterionic transition states. Consequently, the crossing of the S_1 and S_0 surfaces is removed in polar solvents.

The idea that the properties of a conical intersection can be controlled by electrostatic interactions was recently discussed.[11,12] In these papers, it was suggested that the energy of the conical intersection can be controlled by electrostatic interactions with solvents when the degenerate point is created by crossing of two states of different polarities. The present case shows that under certain conditions the degeneracy can be actually lifted by solvent interactions.

According to the quantum-chemical model calculations on CPDHP, at the conical intersection (or the avoided crossing, in the case of polar solvents), the two rings are perpendicular to each other, whereas the minimum structure of the system is planar. According to the Frank−Condon principle, photon absorption is a vertical process; thus, the excited state structure produced immediately after photon absorption will also be planar. Quantum-mechanical calculations on the first excited state show that the torsion mode is practically barrier-less on the first excited state, and the conical intersection is the lowest point on first excited state potential energy surface in the gas phase and in nonpolar solvents; in more polar solvents, the degeneracy disappears and the gap between the states increases with the polarity of the solvent. This means that experimental observables such as quantum yield of fluorescence and decay time of the excited state are expected to increase as the polarity of the solvent increases. Moreover, the model predicts that if the torsional motion is inhibited, for instance in a rigid environment, then the molecule is likely to fluoresce, as it cannot reach the conical intersection.

V. Discussion

Several experimental observations show that the ultrafast decay of the excited singlet state of BIDP in liquid solutions at room temperature is due to efficient internal conversion. In contrast, in glassy solutions at cryogenic temperatures, the fluorescence yield is quite large: 0.59 in MeCN and around 0.1 in nonpolar solvents. Interestingly, the non-radiative processes competing with fluorescence appear to be more effective in nonpolar solvents even in the glassy environment. At this point, we can only speculate as to the non-radiative process(es) responsible for this finding. As no net chemical reaction takes place, they may be due to intersystem crossing and perhaps also internal conversion, or to the presence of aggregates that can serve as low energy traps.[34] The data strongly suggest that a large amplitude motion is required for the internal conversion process; the most likely candidate is torsion around the central C═C bond, a coordinate that leads to E/Z isomerization. Similar observations have been made in other systems capable of this reaction such as stilbene,[35,36] retinal,[37] and the green fluorescence protein (GFP) chromophore.[38] However, this is the first detailed study of the solvent effect on the ultrafast decay in this system.

In distinction with these latter systems, a novel finding is that the room temperature decay is almost an order of magnitude faster in nonpolar solvents than in polar ones. This is in agreement with a theoretical model that predicts the existence of a conical intersection for the smaller but electronically similar CPDHP in nonpolar solvents and therefore an efficient funnel for S_1/S_0 internal conversion. In polar solvents, the model predicts a gap between the two singlet states, that is, elimination of the state crossing. Quantum-chemical calculations on the smaller molecule confirm numerically the model's predictions. According to the model, the S_0 and S_1 surfaces approach each other along two coordinates: torsion around the central C═C bond and aromatization (Figure 8). The curves are found to cross in the gas phase and in cyclohexane, but in a polar solvent, a gap of about 0.5 eV is calculated. The large amplitude motion that is blocked in glassy solutions is, according to the model, the torsion. The ultrafast decay in nonpolar solvents is assigned to the very close proximity of S_0 and S_1 at the perpendicular geometry. The decay in a polar solvent, although slower than in the nonpolar ones, is still very rapid. Apparently, the larger gap calculated for these solvents (~0.5 eV) is nevertheless small enough for the system to cross efficiently from S_1 to S_0.

An apparently similar solvent effect on the lifetime of an electronically excited state was reported by Gustavsson et al

for uracil and fluoro-uracyl.[8,9] It was found that the ultrafast decay of the electronically excited state is much shorter (by a factor of 4) in MeCN than in water which is more polar and also can form hydrogen bonds. In the comprehensive quantum mechanical study of solvent effects on the behavior of the system, it was argued that the solvent modifies the electronic structure of the molecule. However, the explanation proposed by the authors for the solvent effect is completely different from the one presented here. In the case of uracil, there is a conical intersection connecting the fluorescent S_π state with the ground state, accounting for the fast decay in both solvents. The more efficient decay in MeCN was explained by the existence of a second conical intersection between the S_π state and a dark S_n state. Thus, the similarity is only apparent as the physics of the two systems are significantly different.

VI. Summary

Previous work from this group predicted a strong correlation between transition states on the ground state surface and an S_0/S_1 conical intersection.[17,18] Stabilization of a polar transition state by electrostatic interactions is therefore predicted to affect also the energy of a conical intersection and, in extreme cases, to eliminate the degeneracy altogether. In the present combined experimental and theoretical paper, a molecular system with the required properties was designed and synthesized, and its photophysical properties were studied in fluid and frozen solutions. The most important novel result is that in the solid solutions the molecule is strongly fluorescent, in sharp contrast with the case of fluid solutions. The most likely explanation is the hindrance of the torsional motion that is required to attain the conical intersection. No major change in the electronic structure of the excited state is expected upon freezing the solutions. In fact, in a frozen solution the apparent polarity of polar solvents is reduced,[39,40] since the rotational and translational motions required to change the solvation layer are also prohibited. In contrast with previous studies,[8,9] the polar solvent used at room temperature (MeCN) cannot form hydrogen bonds; its effect must be due only to the higher polarity. In line with the model, the S_1 state was found to have an ultra-short decay time in the fluid solvents, indicating the existence of a conical intersection. A strong solvent effect on the lifetime was found; the decay was faster in nonpolar solvents than in polar ones. The fact that even in the absence of actual curve crossing (in polar solvents) k_{IC} of the excited state is relatively large (only a factor of 6–7 smaller than when a crossing occurs) implies that avoided crossings can also act as funnels when the energy gap is small.

Acknowledgment. We are indebted to Professor Omar Deeb and Ms. Shirin Al-Falah for many discussions and for helping in the calculations, and we thank Dr. L. Lustres, Professor N. Ernsting and Professor Israel Agranat for some most enlightening discussions. The Minerva Farkas Center for Light Induced Processes is supported by the Minerva Gesellschaft mbH.

Supporting Information Available: Fluorescence of BIDP. This information is available free of charge via the internet at http://pubs.acs.org.

References and Notes

(1) Teller, E. *J. Phys. Chem.* **1937**, *41*, 109.
(2) *Conical Intersections: Electronic Structure, Dynamics and Spectroscopy*; W Domcke, W.; Yarkony, D. R.; Köppel, H. Eds. World Scientific: Singapore, 2004.
(3) A recent Faraday discussion provided a good coverage of the state of the field: *Faraday Dis.* 2004, Vol. 127.
(4) Fuss, W.; Kosmidis, C.; W. E. Schmid, W. E.; Trushin, S. A. *Angew. Chem., Int. Ed.* **2004**, *43*, 4178.
(5) Espagne, A.; Paik, D. H.; Changenet-Barret, P.; Martin, M. M.; Zewail, A. H. *ChemPhysChem* **2006**, *7*, 1717.
(6) Crespo-Hernandez, C. E.; Cohen, B.; Hare, P. M.; Kohler, B. *Chem. Rev.* **2004**, *104*, 1977.
(7) Canuel, C.; Elhanine, M.; Mons, M.; Piuzzi, F.; Tardivel, B.; Dimicoli, I. *Phys. Chem. Chem. Phys.* **2006**, *8*, 3978.
(8) Gustavsson, T.; Sarkar, N.; Lazzarotto, E.; Markovitsi, D.; Barone, V.; Improta, R. *J. Phys. Chem. B* **2006**, *110*, 12843.
(9) Gustavsson, T.; Sarkar, N.; Lazzarotto, E.; Markovitsi, D.; Improta, R. *Chem. Phys. Lett.* **2006**, *429*, 551.
(10) Santoro, F.; Barone, V.; Gustavsson, T.; Improta, R. *J. Am. Chem. Soc.* **2006**, *128*, 16312.
(11) Burghardt, I.; Cederbaum, L. S.; Hynes, J. T. *Faraday Dis.* **2004**, *127*, 395.
(12) Toniolo, A.; Olsen, S.; Manohar, L.; Martinez, T. J. *Faraday Dis.* **2004**, *127*, 149.
(13) Gustavsson, T.; Banyasz, A.; Lazzarotto, E.; Markovitsi, D.; Scalmani, G.; Frisch, M. J.; Barone, V.; Improta, R. *J. Am. Chem. Soc.* **2006**, *128*, 607.
(14) Altoe, P.; Bernardi, F.; Garavelli, M.; Orlandi, G.; Negri, F. J. *J. Am. Chem. Soc.* **2005**, *127*, 3952.
(15) Cogan, S.; Haas, Y. *J. Photochem. Photobiol. A* **2008**, *193*, 25.
(16) See for instance Yang, J. S.; Liau, K. L.; Tu, C. W.; Hwang, C. Y. *J. Phys. Chem. A* **2005**, *109*, 6450.
(17) Haas, Y.; Cogan, S.; Zilberg, S. *Int. J. Quant. Chem.* **2005**, *102*, 961–970.
(18) Haas, Y.; Zilberg, S. *Adv. Chem. Phys.* **2002**, *124*, 433.
(19) Zilberg, S.; Haas, Y. *Eur. J. Chem.* **1999**, *5*, 1755.
(20) (a) Berson, J. A.; Evleth, E. M.; Hamlet, Z. *J. Am. Chem. Soc.* **1965**, *87*, 2887. (b) Boyd, G. V.; Ellis, A. W.; Harms, M. D. *J. Chem. Soc. C* **1970**, 800.
(21) Schmidt, M.W.; Baldridge, K. K.; Boatz, J. A.; Elbert, S. T.; Gordon, M. S.; Jensen, J. J.; Koseki, S.; Matsunaga, N.; Nguyen, K. A.; Su, S.; Windus, T. L.; Dupuis, M.; Montgomery, J. A. *J. Comput. Chem.* **1993**, *14*, 1347.
(22) Schmidt, M. W.; Gordon, M. S. *Ann. Rev. Phys. Chem.* **1998**, *49*, 233.
(23) Dunning, J. T. H.; Hay, P. J. In *Methods of Electronic Structure Theory*; Schaefer, H. F., III, Ed.; Plenum Press: New York, 1977; Chapter 1, 1–27.
(24) Jones, G.; Jackson, W. R.; Choi, C.; Bergmark, W. R. *J. Phys. Chem.* **1985**, *89*, 294.
(25) Kulander, K. C.; Heller, E. J. *J. Chem. Phys* **1978**, *69*, 2439.
(26) Myers, A. B.; Mathies, R. A.; In *Biol. Appl. Raman Spectrosc.*; Spiro, T. G., Ed.; Wiley: New York, 1987; Vol. 2, p 1.
(27) Myers, A. B.; Mathies, R. A.; Tannor, D. J.; Heller, E. J. *J. Chem. Phys.* **1982**, *77*, 3857.
(28) Strickler, S. J.; Berg, R. A. *J. Chem. Phys.* **1962**, *37*, 814.
(29) Kirkwood, J. *J. Chem. Phys.* **1934**, *2*, 351.
(30) Onsager, L. *J. Am. Chem. Soc.* **1936**, *58*, 1486.
(31) Miertus, S.; Scrocco, E.; Tomasi, J. *Chem. Phys.* **1981**, *55*, 117.
(32) The figure shows a search for the conical intersection along a single coordinate, although two coordinates are generally required (see ref 15). If a symmetry element is conserved along a phase inverting reaction path between two critical points and the two crossing states belong to different irreducible representations, a one-dimensional search is sufficient. The reason is that the derivative of the electronic Born−Oppenheimer Hamiltonian with respect to any symmetry-preserving coordinate is a totally symmetric operator. All matrix elements of this operator between states of different irreducible representations and hence the coupling V vanish. This is the case: both transition states belong to C_{2V} symmetry, the biradical TS transforms as a_2 and the zwitterion TS as a_1. The coordinate connecting the two transition states is a phase inverting one and the conserved symmetry element is the C_2 rotation.
(33) Hammond, G. S. *J. Am. Chem. Soc.* **1955**, *77*, 334.
(34) We are indebted to one of the reviewers for a discussion of this point.
(35) Saltiel, J.; Waller, A. S.; Sears, D. F., Jr. *J. Am. Chem. Soc.* **1993**, *115*, 2453.
(36) Todd, D. C.; Fleming, G. R. *J. Chem. Phys.* **1993**, *98*, 269.
(37) Hou, B.; Friedman, N.; Ruhman, S.; Ottolenghi, M. *J. Phys. Chem. B* **2001**, *105*, 7042.
(38) Webber, N. M.; Litvinenko, K. L.; Meech, S. R. *J. Phys. Chem. B* **2001**, *105*, 8036.
(39) Wallacher, D.; Soprunyuk, V. P.; Knorr, K.; Kityk, A. V. *Phys. Rev. B* **2004**, *69*, 134207.
(40) Ibberson, R. M.; David, W. I. F.; Yamamuro, 0.; Miyoshi, Y.; Matsuo, T.; Suga, H. *J. Phys. Chem.* **1995**, *99*, 14167.

JP7110296